Coherent control of temporal pulse shaping by electromagnetically induced transparency

Roberto Buffa,[1] Stefano Cavalieri,[2] and Marco V. Tognetti[1]
[1]*Dipartimento di Fisica, Università di Siena, and Istituto Nazionale per la Fisica della Materia, Via Roma 56, I-53100 Siena, Italy*
[2]*Dipartimento di Fisica, and European Laboratory for Nonlinear Spectroscopy, Università di Firenze, and Istituto Nazionale per la Fisica della Materia, Via G. Sansone 1, I-50019 Sesto Fiorentino, Italy*
(Received 12 July 2003; published 22 March 2004)

We present the coherent control of the temporal shape of laser pulses obtained by exploiting the propagation dynamics of electromagnetically induced transparency. Temporal compression, as a special case of pulse tailoring, is discussed. We envisage applications in nonlinear optics processes and control of pulse shapes in the vacuum ultraviolet spectral region.

DOI: 10.1103/PhysRevA.69.033815 PACS number(s): 42.50.Gy, 32.80.Qk, 42.50.Hz

Electromagnetically induced transparency (EIT) is a coherent interaction process in which a coupling laser field is used to modify the optical properties of an atomic medium at the frequency of a probe laser field [1]. Since its discovery the process has received a lot of attention and the reader is referred to the most recent review article [2] for an exhaustive list of papers related to EIT. In the last few years research has been focused on the propagation of light pulses in EIT modified media [3]. Most notably, from the point of view of the work discussed here, particular attention has been devoted to ultraslow light propagation [4,5] and light storage techniques [6–8]. In this regard, EIT can be viewed as a way of coherently controlling the propagation velocity of the probe laser pulse as described by the dark-state polaritons approach [6]. Experimental evidence of the possibility to control also the temporal shape of the probe pulse has been recently reported by Chien Liu *et al.* [8].

In this paper we present a theoretical study which discusses and explains how to exploit the peculiarities of EIT propagation dynamics to coherently control the temporal shape of the probe laser pulse. We will show how the control is indeed possible by a proper choice of the temporal shape of the coupling laser pulse. Besides its fundamental interest, this pulse shaping technique, when applied to the vacuum ultraviolet (VUV) spectral region, can have also important applications.

Figure 1 shows a schematic diagram of the physical system at the basis of EIT: a three-level atom in interaction with two laser pulses, of electric-field envelopes E_p (probe) and E_c (coupling), and frequencies ω_p and ω_c, resonant with the atomic transitions 1-3 and 2-3, respectively. While keeping the formulation general, we have in mind the case of a rare-gas atom, where ω_p is in the VUV and ω_c is in the visible or infrared spectral region.

Figure 2 shows in a heuristic way the idea at the basis of this paper. The laser pulses, propagating along the z axis, enter the cell of length L containing the medium of three-level atoms with the temporal overlapping shown in (a). The probe pulse experiences EIT and its propagation velocity v_p slows down to a value $v_p=(1/c+k/E_c^2)^{-1}$ [1,2]. As a result, after some propagation in the cell, the coupling pulse overlaps the probe pulse as shown in (b). In this condition, different "points" of the probe pulse experience different values of E_c and "travel" with different "propagation velocity," giving rise to a temporal reshaping of the probe pulse. A proper choice of the temporal shape of the coupling pulse is expected to result in a control of the temporal shape of the probe pulse.

In a rigorous approach, the propagation equations of the electric-field envelopes E_p and E_c are written as

$$\left(\frac{\partial}{\partial z}+\frac{1}{c}\frac{\partial}{\partial t}\right)E_p=-jN\frac{\omega_p d_{13}}{2\varepsilon_0 c}\rho_{31},$$
$$\left(\frac{\partial}{\partial z}+\frac{1}{c}\frac{\partial}{\partial t}\right)E_c=-jN\frac{\omega_c d_{23}}{2\varepsilon_0 c}\rho_{32}, \tag{1}$$

where N is the density of the atomic sample and d_{n3} is the electric-dipole moment of the n-3 transition. For a weak probe field ($\rho_{11}\approx 1$), the coherences ρ_{nm} that appear in Eq. (1) satisfy the following equations:

$$\dot{\rho}_{21}=-j\Omega_c\rho_{31}-\gamma_{21}\rho_{21},$$
$$\dot{\rho}_{31}=-j\Omega_p-j\Omega_c\rho_{21}-\gamma_{31}\rho_{31}, \tag{2}$$
$$\dot{\rho}_{32}=0,$$

where $\Omega_p=d_{13}E_p/2\hbar$ and $\Omega_c=d_{23}E_c/2\hbar$ are the Rabi frequencies of the atomic transitions, and γ_{nm} represents all kinds of dephasing rates. When

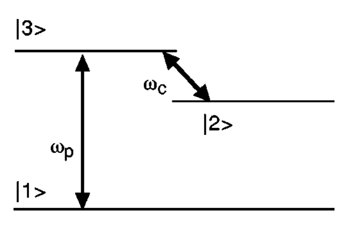

FIG. 1. Schematic diagram of the three-level atomic system at the basis of EIT.

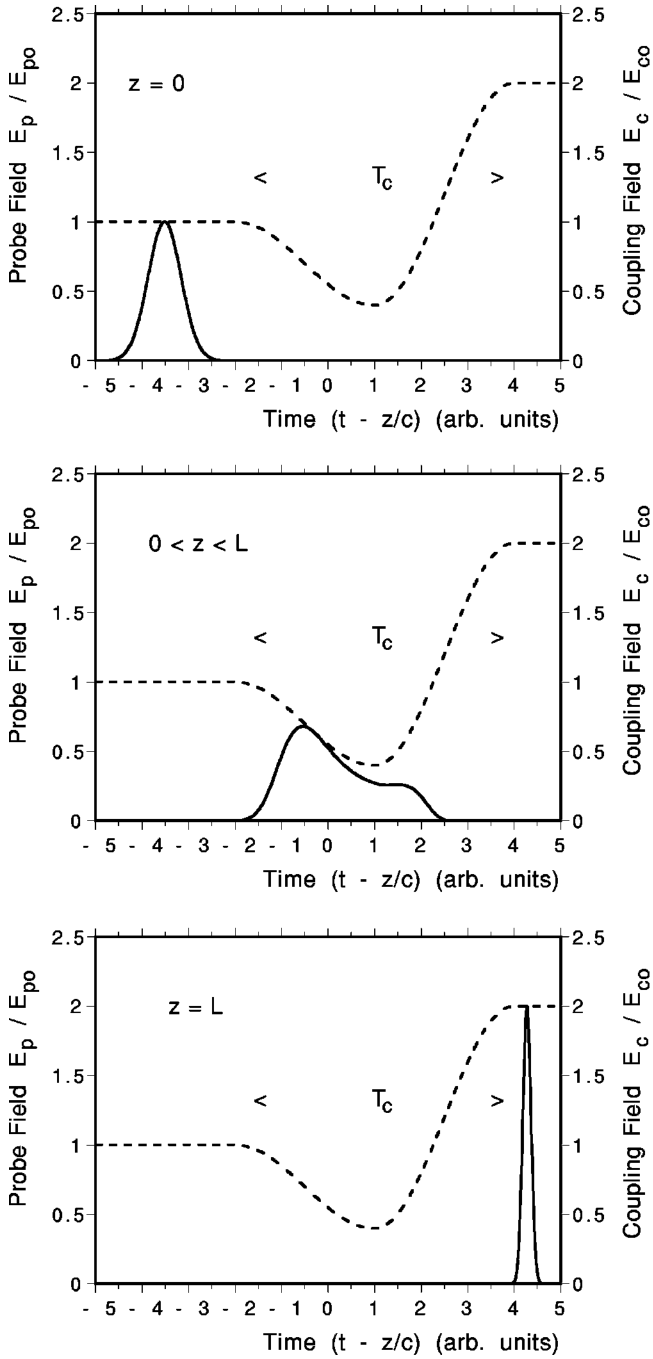

FIG. 2. The idea at the basis of the temporal shape control. In the framework moving at velocity c, the probe pulse (continuous line) is slipping under the coupling pulse (dashed line) inside a cell containing the EIT modified medium. Different "points" of the probe pulse "travel" at different "propagation velocity" resulting in a reshaping of the probe pulse temporal profile.

$$\Omega_c \gg \gamma_{31}, \dot{\Omega}_c/\Omega_c, \dot{\Omega}_p/\Omega_p \tag{3a}$$

and

$$\dot{\Omega}_p/\Omega_p \gg \gamma_{21}, \tag{3b}$$

the solution of Eq. (2) is given by

$$\rho_{21} = -\frac{\Omega_p}{\Omega_c},$$

$$\rho_{31} = j\left[\frac{\dot{\Omega}_c}{\Omega_c^3}\Omega_p - \frac{\dot{\Omega}_p}{\Omega_c^2}\right], \tag{4}$$

$$\rho_{32} = 0.$$

Then, the introduction of Eq. (4) in Eq. (1) provides the following propagation equations [6]:

$$\frac{\partial}{\partial z}E_p + \frac{1}{c}\frac{\partial}{\partial t}E_p = -\frac{\kappa}{E_c}\frac{\partial}{\partial t}\left(\frac{E_p}{E_c}\right),$$
$$\frac{\partial}{\partial z} + \frac{1}{c}\frac{\partial}{\partial t}E_c = 0, \tag{5}$$

whose solution can be written as

$$E_p(z,t) = \frac{E_{p0}}{E_{c0}}E_c(t-z/c)f(\xi(z,t)),$$
$$E_c(z,t) = E_c(t-z/c), \tag{6}$$

with

$$\xi(z,t) = z - \int_{z/c}^{t-z/c}\frac{E_c^2(t'-z/c)}{\kappa}dt',$$

and where

$$\kappa = N\frac{\hbar\omega_p}{\varepsilon_0 c}\left(\frac{d_{13}}{d_{23}}\right)^2,$$

E_{p0} and E_{c0} are constants, and $f(\xi)$ is a function which guarantees the boundary conditions for E_p at $z=0$ [9].

A condition which provides a straightforward analytical solution is provided by a probe field E_p that, at $z=0$, is overlapped by a flat region of E_c as, for instance, it is shown in Fig. 2(a). Then Eq. (6) provides the analytical expression of $f(\xi)$ and the following equation:

$$E_p(z,t) = \frac{E_c(t-z/c)}{E_{c0}}E_p\left(0, -\frac{\kappa}{E_{c0}^2}\xi(z,t)\right). \tag{7}$$

The analysis of Eq. (7) shows that the evolution of E_p is governed by the temporal profile of E_c and by the dimensionless parameter

$$\alpha = \frac{NL}{T_p}\frac{\hbar\omega_p}{\varepsilon_0 c E_{c0}^2}\left(\frac{d_{13}}{d_{23}}\right)^2,$$

where T_p is a characteristic time of the probe pulse. Equation (7) suggests how it is possible to control the temporal shape of the probe pulse. In fact, given the expression of $E_p(0,t)$ and a target pulse $E_T(t)$, then Eq. (7) represents an implicit equation that can be solved by numerical procedures to provide the expression of $E_c(t-z/c)$ which gives at the cell output $E_p(L,t)=E_T(t)$. The validity of the solution (7), when conditions (3a) and (3b) are satisfied, has been checked by

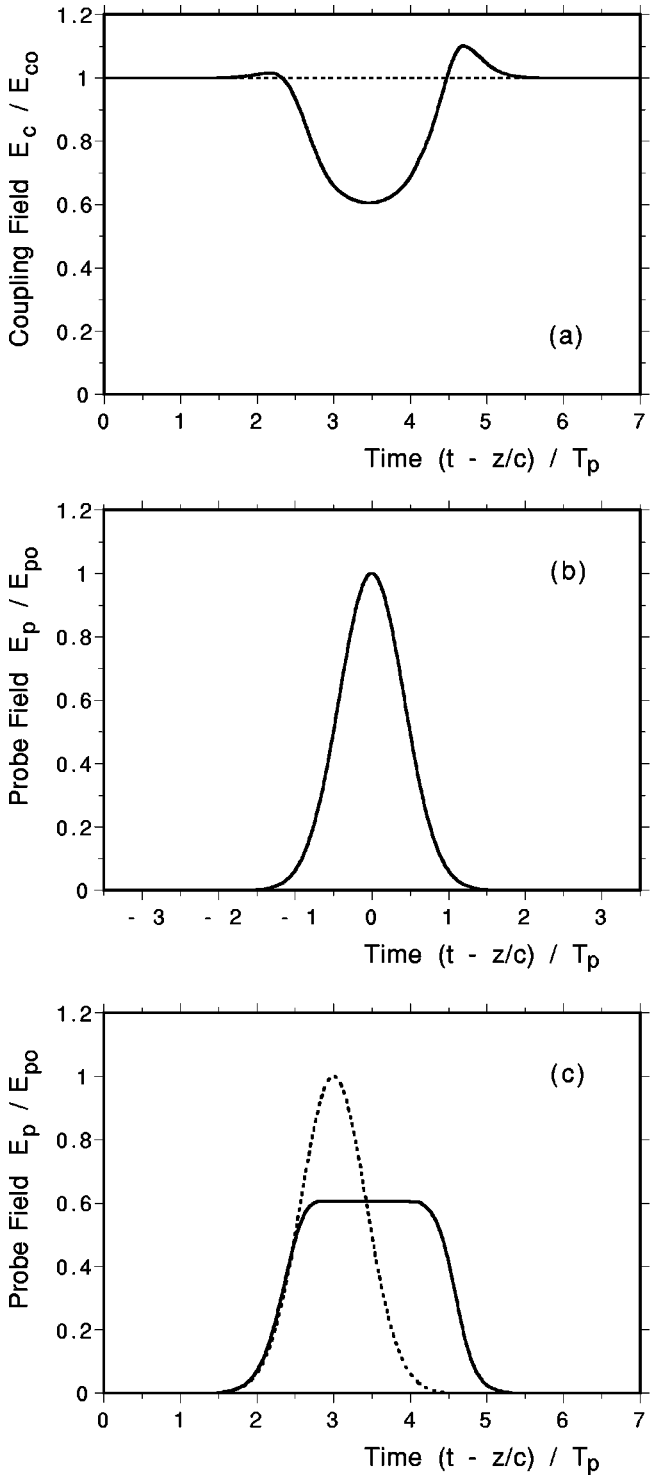

FIG. 3. Temporal shape control: flat-top pulse. (a) Coupling pulse, (b) probe pulse at $z=0$, (c) probe pulse at $z=L$. The dashed line in (c) shows the output probe pulse when the coupling field is taken constant [$E_c=E_{c0}$, dashed line in (a)].

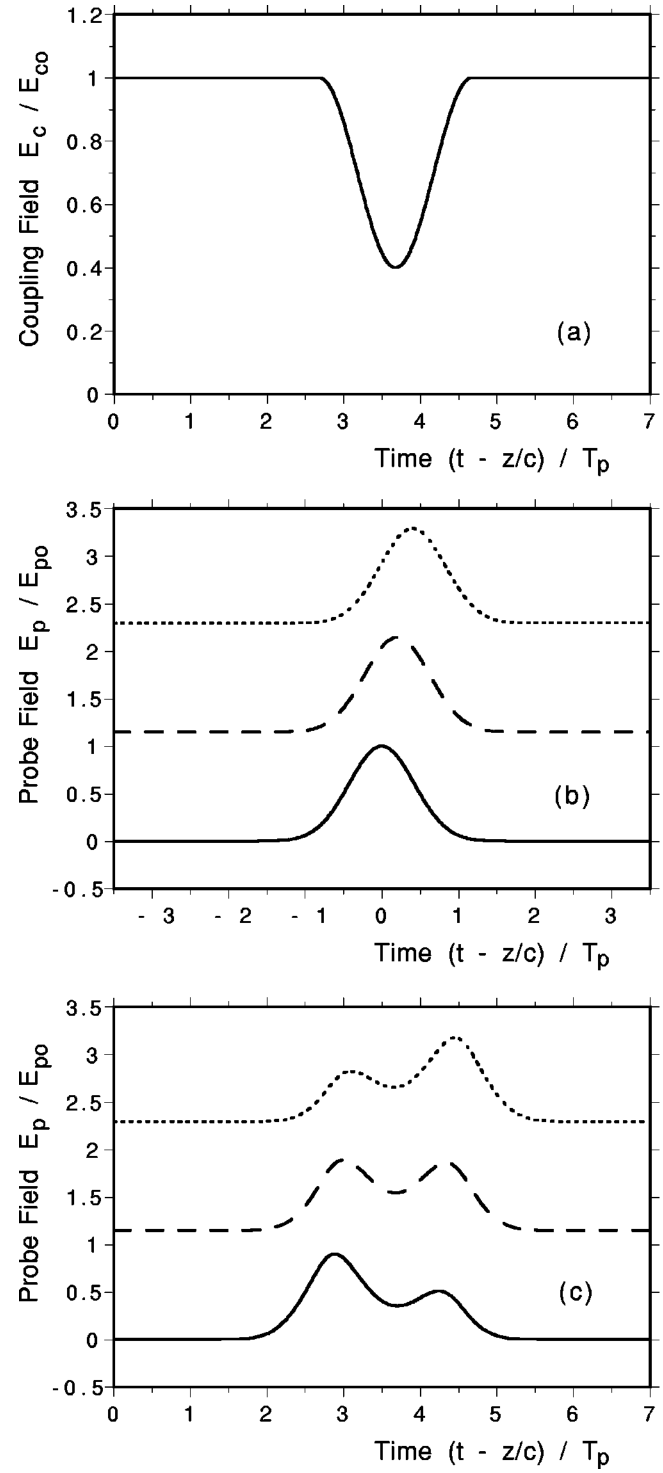

FIG. 4. Temporal shape control: two-peaked pulse. (a) Coupling pulse, (b) input probe pulses with various delays with respect to the coupling pulse, (c) corresponding output probe pulses. In (b) and (c) plots are vertically shifted for the sake of clarity.

direct numerical integration of the Maxwell-Bloch equations (1) and (2). The limit of validity of Eq. (7), when conditions (3a) and (3b) are not strictly satisfied, as well as the possibility of arbitrary temporal tailoring of the probe pulse are at present time under investigation.

In Figs. 3 and 4 we present a few examples to show the potentiality of the technique discussed. For the results presented we have checked that the numerical solution of the Maxwell-Bloch equations (1) and (2) and the analytical expression (7) provide exactly the same results. Figure 3(a) shows the temporal shape of the coupling pulse that, in the condition $\alpha=3$, provides at the cell output the flat-top probe pulse shown in Fig. 3(c) when a Gaussian probe pulse of temporal width T_p is taken at the cell input (b). For an easy comparison, the Gaussian probe pulse obtained at the cell output when the coupling field is taken constant ($E_c = E_{c0}$) is also shown by the dashed line.

Figure 4 shows how different temporal shapes of the probe pulse at the cell output (c) are obtained with the same temporal shape of the coupling pulse (a) by simply changing the relative pulse delay at the cell input (b) ($\alpha=3$).

Pulse compression appears as a special case of temporal shaping. In fact, if at the cell output a flat region of $E_c = nE_{c0}$ overlaps E_p such as, for instance, it is shown in Fig. 2(c), then Eq. (7) provides

$$E_p(L,t) = nE_p(0,n^2(t-t_L)), \tag{8}$$

where t_L, defined implicitly through

$$L = \int_{L/c}^{t_L - L/c} \frac{E_c^2(t'-L/c)}{\kappa} dt',$$

is the arrival time of the probe pulse peak at $z=L$. Equation (8) shows how the probe pulse, while preserving its functional shape, is temporally compressed by a factor n^2 and its amplitude amplified by a factor n. No need to say that when $n<1$, then the probe pulse is temporally broadened and its amplitude reduced. This result explains in a straightforward way the experimental observations reported by Chien Liu *et al.* [8]. It is worthwhile stressing that, provided that approximations (3a) and (3b) are fulfilled, and that flat regions of the coupling pulse E_c overlap the probe pulse E_p at the cell input and output, then the compression factor n^2 is independent of any characteristic time scale of the involved levels, and it is independent of the detailed temporal structure of the coupling pulse. The result obtained can have important applications for processes of nonlinear optics in the VUV. In fact, the use of the output compressed pulse as a light source can greatly increase the efficiency of a subsequent nonlinear process.

For a constant coupling field, EIT shows a finite transparency spectral bandwidth, proportional to

$$\Delta\omega = \left[N \frac{d_{13}^2 \omega_p}{8\hbar c \varepsilon_0} \frac{\gamma_{31}}{\Omega_c^4} L \right]^{-1/2},$$

which sets a limit to the temporal duration of the probe pulse that can travel in the medium without absorption. The limit of the compression factor that can be achieved for a given value of the parameter α is at present time under investigation. To provide here a realistic example, we have checked by direct numerical integration of the Maxwell-Bloch equations (1) and (2) that, taking standard atomic parameters ($d_{13}=4.8\times10^{-30}$ Cm, $d_{23}=9.5\times10^{-30}$ Cm, $1/\gamma_{21} \gg 1/\gamma_{31} = 30$ ns, $\hbar\omega_p = 8.3\times10^{-19}$ J, $\hbar\omega_c = 4.0\times10^{-19}$ J) [10], and using standard laboratory conditions ($N=10^{15}$ atoms/cm^3, $L=5$ cm), a probe laser pulse of temporal duration (full width at half maximum) $T_p=10$ ns is temporally compressed by a factor $n^2=10$ by a coupling field with $E_{c0} = 1.5\times10^5$ V/m and $T_c=30$ ns (see Fig. 1), showing no absorption. With these values, the transparency spectral bandwidth of the medium $\Delta\omega$ results to be an order of magnitude larger than the spectral bandwidth $\delta\omega$ of the compressed probe pulse. This example indicates the feasibility of the discussed scheme under considerably relaxed experimental conditions.

In conclusion, we have shown that temporal pulse shaping and compression can be achieved using EIT schemes under considerably relaxed experimental conditions. The process presents both fundamental interest and applications to VUV nonlinear processes and control of VUV pulse shapes. In fact it offers the possibility of temporal tailoring of short wavelength light pulses by a proper choice of a control field in the visible or infrared spectral region, where pulse shaping is feasible.

[1] S. E. Harris, Phys. Today **50**(7), 36 (1997).
[2] J. P. Marangos, J. Mod. Opt. **45**, 471 (1998).
[3] P. W. Milonni, J. Phys. B **35**, 31 (2002).
[4] A. Kasapi, M. Jain, G. Y. Yin, and S. E. Harris, Phys. Rev. Lett. **74**, 2447 (1995).
[5] L. V. Hau, S. E. Harris, Z. Dutton, and C. H. Behroozi, Nature (London) **397**, 594 (1999).
[6] M. Fleischhauer and M. D. Lukin, Phys. Rev. Lett. **84**, 5094 (2000).
[7] D. F. Phillips, A. Fleischhauer, A. Mair, R. L. Walsworth, and M. D. Lukin, Phys. Rev. Lett. **86**, 783 (2001).
[8] Chien Liu, Z. Dutton, C. H. Behroozi, and L. V. Hau, Nature (London) **409**, 490 (2001).
[9] If E_c overlaps E_p Eq. (6) satisfies the condition $(\partial/\partial z)\int_{-\infty}^{+\infty} E_p^2(z,t)dt = 0$ which shows how the energy flux of the probe pulse remains constant.
[10] R. Buffa, M. P. Anscombe, and J. P. Marangos, Phys. Rev. A **67**, 033801 (2003).